4. Absorption spectra

When a GNR is under the influence of an electromagnetic field with polarization $\hat{\mathbf{e}}\|\hat{x}$, the absorption spectrum $A(\omega)$ for direct photon transitions ($\Delta k_x = 0$) from the initial state $|\Psi^h(k_x, J^h)\rangle$ to the final state $|\Psi^{h'}(k_x, J^{h'})\rangle$ is given by

$$A(\omega) \propto \sum_{J^h, J^{h'}} \int_{\text{1st B.Z.}} \frac{\mathrm{d}k_x}{2\pi} \left| \langle \Psi^{h'}(k_x, J^{h'}) | \frac{\hat{\mathbf{e}} \cdot \mathbf{p}}{m_e} | \Psi^h(k_x, J^h) \rangle \right|^2 \times \mathrm{Im} \left\{ \frac{f[E^h(k_x, J^h)] - f[E^{h'}(k_x, J^{h'})]}{E^{h'}(k_x, J^{h'}) - E^h(k_x, J^h) - \omega - i\Gamma} \right\}, \tag{10}$$

where m_e is the effective mass of an electron, $\mathbf{p}$ is the momentum operator, $f[E^h(k_x, J^h)]$ is the Fermi-Dirac distribution function, and Γ is the broadening factor. The low-energy absorption spectra for the $N_y = 69$ AGNR and ZGNR at zero temperature are illustrated in Fig. 4. The spectra show a lot of 1D peaks caused by the inter-band transitions of the 1D subbands, and they are greatly affected by the geometric structure.

In the absorption spectrum of the $N_y = 69$ AGNR [Fig. 4(a)], the first peak, located at $\omega_1 = 0.055\ \gamma_0$, is identified as the excitation from the $J^v = 1$ to the $J^c = 1$ subband. The second ($\omega_2 = 0.105\ \gamma_0$) and the third ($\omega_3 = 0.205\ \gamma_0$) ones are the transitions from the $J^v = 2$ to the $J^c = 2$ subband and from the $J^v = 3$ to the $J^c = 3$ subband, respectively. The allowed transitions originate in the subbands of the same indices, i.e., the selection rule is $\Delta J = J^c - J^v = 0$. The transition energy is twice the band-edge energy ($\omega_J = 2E^{edge}_{J^c} = 2|E^{edge}_{J^v}|$, where $J^c = J^v = J$) because the band structure is symmetric about $E_F = 0$. Moreover, the peak height increases when the frequency increases as a consequence of the decrease of the subbands' curvatures.

For ZGNRs, the absorption peaks may be classified into principal peaks and subpeaks based on their heights, as shown in Fig. 4(b). The allowed transitions obey the selection rule $|\Delta J| = odd$, which is different from the armchair case, $\Delta J = 0$. The principal peaks become higher with increasing frequency because of the decrease of the bands' curvatures and the increase of the excitation channels. Due to the symmetry of the energy spectrum, the absorption spectrum of negative ΔJ's is the same as that of positive ones. Therefore, only the positive ΔJ cases (transitions from the J^v to the $J^c = J^v + \Delta J$ subband of energy $\omega = E^{edge}_{J^v+\Delta J} - E^{edge}_{J^v}$) are discussed. The principal peaks, ω^P_J, are contributed by transitions between subbands satisfying the selection rule $\Delta J = 1$ ($J^v \to J^c : 1 \to 2$), $\Delta J = 1$ ($J^v \to J^c : 2 \to 3$), $\Delta J = 1, 3$ ($J^v \to J^c : 3 \to 4,\ 2 \to 5$), $\Delta J = 1, 3, 5$ ($J^v \to J^c : 4 \to 5,\ 3 \to 6,\ 2 \to 7$), and so on. The corresponding numbers of excitation channels are 2, 2, 4, and 6, i.e., double of the allowed positive ΔJ number. On the other hand, there exists one subpeak between two adjacent principal peaks. These subpeaks are indicated by ω_{1J}, where the subscript $1J$ denotes the transition from the $J^v = 1$ valence subband to the J^c conduction subband. The subpeak ω_{14}, for instance, results from the transition between the $J^v = 1$ and the $J^c = 4$ subband and follows the optical selection rule $\Delta J = 3$. Since each subpeak possesses two excitation channels, the increase of subpeak height is not as rapid as the height increase of principal peaks. It is remarkable that only the first principal peak (ω^P_1) and all the subpeaks (ω_{1J}) are derived from the transitions related to the $J^{c,v} = 1$ subbands ($E_{J^{c,v}=1} = E_F = 0$). The ω^P_1 peak is located at $E^{edge}_{J^c=2}$, and the subpeaks ω_{1J} are positioned at $E^{edge}_{J^c=J}$, which is the energy difference between the subband edge and the Fermi level.

#153227 - $15.00 USD Received 22 Aug 2011; revised 8 Oct 2011; accepted 8 Oct 2011; published 1 Nov 2011

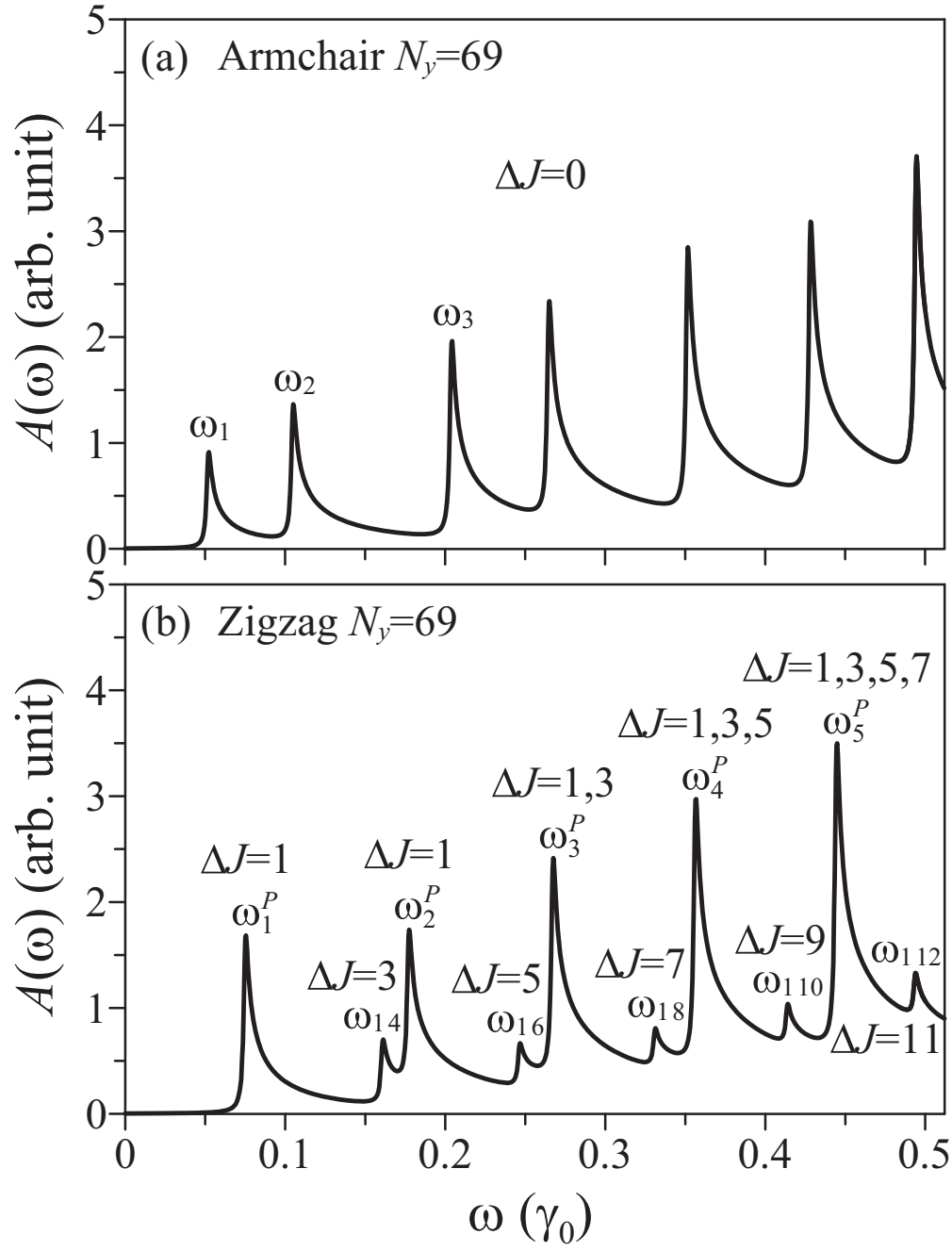

Fig. 4. Absorption spectra for the $N_y = 69$ AGNR and ZGNR.

#153227 - $15.00 USD Received 22 Aug 2011; revised 8 Oct 2011; accepted 8 Oct 2011; published 1 Nov 2011

5. Optical absorption selection rules of GNRs

Based on the above-discussed features of wavefunctions, the optical selection rules are also determined by the velocity matrix elements [the former term in Eq. (10)], which are defined as

$$M^{hh'}(k_x) \equiv \langle \Psi^{h'}(k_x, J^{h'}) | \frac{\hat{\mathbf{e}} \cdot \mathbf{p}}{m_e} | \Psi^{h}(k_x, J^{h}) \rangle. \tag{11}$$

To evaluate $M^{hh'}$, the momentum operator is substituted in terms of the k-space derivative of the Hamiltonian [41–44]:

$$\mathbf{p}(\mathbf{k}) = \frac{m_e}{\hbar} \nabla_{\mathbf{k}} H(\mathbf{k}). \tag{12}$$

This substitution is valid independent of the band-structure model. Thus, it is equally applicable and straightforward to use for any empirical approach for the electronic dispersion relation [44], so that

$$M^{hh'}(k_x) = \frac{1}{\hbar} \sum_{l,l'=1}^{2N_y} C_l^{h'*}(k_x) C_{l'}^{h}(k_x) \frac{\partial H_{l,l'}(k_x)}{\partial k_x}, \tag{13}$$

where $\hbar$ is treated as unity in the following derivation.

At zero temperature, only the inter-band transitions from the valence to the conduction subbands are valid. To investigate the optical properties, we focus on $k_x = 0$, where the excitations occur for AGNRs. Substituting the coefficients of sublattices B with A in Eq. (13) by the relations $B_m^v = sA_m^v$ ($s = \pm 1$) and $B_m^c = tA_m^c$ ($t = \pm 1$) from Eq. (5), M^{vc} is

$$\begin{aligned}
& b\gamma_0 \sum_{m=1}^{N_y} \Big[-sA_m^{c*}(J^c) A_m^v(J^v) + tA_m^{c*}(J^c) A_m^v(J^v) \Big] \\
+ & \frac{b\gamma_0}{2} \sum_{m=1}^{N_y-1} \Big[-tA_m^{c*}(J^c) A_{m+1}^v(J^v) + sA_m^{c*}(J^c) A_{m+1}^v(J^v) \Big] \\
+ & \frac{b\gamma_0}{2} \sum_{m=2}^{N_y} \Big[-tA_m^{c*}(J^c) A_{m-1}^v(J^v) + sA_m^{c*}(J^c) A_{m-1}^v(J^v) \Big].
\end{aligned} \tag{14}$$

The transfer relations between $A_{m\pm1}$ and A_m, obtained from $H|\Psi\rangle = E|\Psi\rangle$ at $k_x = 0$, are

$$\begin{cases}
A_2 = \Delta_\pm A_1, \\
A_{m-1} + A_{m+1} = \Delta_\pm A_m, \quad \text{if } m = 2, 3, 4, ..., N_y - 1, \\
A_{N_y-1} = \Delta_\pm A_{N_y},
\end{cases} \tag{15}$$

where $\Delta_\pm = \pm(E/\gamma_0) - 1$ for $A_m = \pm B_m$. After using Eq. (15) to replace $A_{m\pm1}$ with A_m, M^{vc} becomes

$$\begin{aligned}
& b\gamma_0 \sum_{m=1}^{N_y} \Big[-sA_m^{c*}(J^c) A_m^v(J^v) + tA_m^{c*}(J^c) A_m^v(J^v) - \frac{\Delta_s}{2} tA_m^{c*}(J^c) A_m^v(J^v) + \frac{\Delta_s}{2} sA_m^{c*}(J^c) A_m^v(J^v) \Big] \\
= & (t-s)(1 - \frac{\Delta_s}{2}) b\gamma_0 \sum_{m=1}^{N_y} A_m^{c*}(J^c) A_m^v(J^v),
\end{aligned} \tag{16}$$

where $\Delta_s = s(E/\gamma_0) - 1$ for $A_m^c = sB_m^c$. Through the relation between the conduction and valence subbands $A_m^v = uA_m^c$ ($u = \pm 1$) from Eq. (6) and the normalization of the wavefunction $2\sum_{m=1}^{N_y} A_m^{c*}(J^c) A_m^c(J^v) = \delta_{J^c,J^v}$, the velocity matrix element at $k_x = 0$ is

$$M^{vc}(k_x = 0) = u(t-s)(1 - \frac{\Delta_s}{2}) b\gamma_0 \frac{1}{2} \delta_{J^c,J^v} = \pm(1 - \frac{\Delta_\pm}{2}) b\gamma_0 \delta_{J^c,J^v},$$

#153227 - $15.00 USD Received 22 Aug 2011; revised 8 Oct 2011; accepted 8 Oct 2011; published 1 Nov 2011

where $\Delta_{\pm} = \pm(E/\gamma_0) - 1$ and $u(t-s)$ is either 0 or ± 2. Eq. (17) yields the selection rule ($\Delta J = 0$) for AGNRs and possible excitation channels in the absorption spectra.

For ZGNRs, the velocity matrix element in Eq. (13) at $k_x = 2\pi/3$, where the transition occur, becomes

$$h' \sum_{m=1}^{N_y} \left[A_m^{c*}(J^c) B_m^v(J^v) + B_m^{c*}(J^c) A_m^v(J^v) \right], \tag{17}$$

where $h' = -a\gamma_0 \sin(\pi a/3)$. For an odd N_y, we use Eq. (8) to convert the second term in Eq. (17), which leads to

$$h' \sum_{m=1}^{N_y} \left[A_m^{c*}(J^c) B_m^v(J^v) + (-1)^{J^c+1} A_{N_y+1-m}^{c*}(J^c)(-1)^{J^v} B_{N_y+1-m}^v(J^v) \right]. \tag{18}$$

Then renaming the index of $N_y + 1 - m$ as m gives

$$[1 + (-1)^{J^c+J^v+1}] h' \sum_{m=1}^{N_y} A_m^{c*}(J^c) B_m^v(J^v). \tag{19}$$

As for an even N_y, the second term in Eq. (18) can also be converted by Eq. (9), and yields the same result as Eq. (19). Hence, the M^{vc} for ZGNR at $k_x = 2\pi/3$ is

$$M^{vc}(k_x = \frac{2\pi}{3}) = \begin{cases} 2h' \sum_{m=1}^{N_y} A_m^{c*}(J^c) B_m^v(J^v), & \text{if } \Delta J = odd, \\ 0, & \text{if } \Delta J = even, \end{cases} \tag{20}$$

where $\sum_{m=1}^{N_y} A_m^{c*}(J^c) B_m^v(J^v)$ has a non-zero value, and the selection rule ($\Delta J = odd$) for ZGNRs is obtained.

By using the selection rules, the transition energies (peak positions) can be efficiently obtained from the energy dispersion. For AGNRs, the dependence of the first five predicted transition energies on the ribbon width is shown in Fig. 5(a). For a certain width N_y, the Jth transition energy is equal to $\omega_J = 2E_{J^c}^{edge}$ ($J^c = J$), i.e., twice of the band-edge state energy of the J^cth subband. For narrower GNRs, there are three groups of transition energies. The ω_J's of $N_y = 3m$ (full circles) and $N_y = 3m+1$ (open circles) groups are very similar, while for the $N_y = 3m+2$ (squares) group, the first and second ω_J's lie close to each other and are sandwiched between the second and third ω_J's of the $N_y \neq 3m+2$ nanoribbons. For wider GNRs, these transition energies make a red-shift and merge. The GNRs may therefore be sorted into the two groups $N_y = 3m+2$ and $N_y \neq 3m+2$. The former is gapless due to the linear bands crossing at the Fermi level, while the latter is semiconducting with a band gap energy corresponding to the first transition energy.

The first five ribbon-width-dependent transition energies of ZGNRs are presented in Fig. 5(b). They are associated with the first principal peak ω_1^P, the first subpeak ω_{14}, the second principal peak ω_2^P, the second subpeak ω_{16}, and the third principal peak ω_3^P, respectively [see Fig. 4(b)]. The predicted corresponding transition energies are $\omega_1^P = E_{J^c=2}^{edge}$, $\omega_{14} = E_{J^c=4}^{edge}$, $\omega_2^P = E_{J^c=3}^{edge} - E_{J^v=2}^{edge}$, $\omega_{16} = E_{J^c=6}^{edge}$, and $\omega_3^P = E_{J^c=4}^{edge} - E_{J^v=3}^{edge}$. The first subpeak ($\omega_{14}$) and the second principal peak (ω_2^P) are close to each other and merge for a sufficiently large width, as to the second subpeak (ω_{16}) and the third principal peak (ω_3^P). In short, the peak frequencies can be predicted by a combination of the band structures and selection rules. This is an efficient way to obtain wide-ranging information on the transition energies without extrapolation.

It is worth mentioning that the exact energies of the band-edge states for ZGNRs can be specified by the experimentally measured transition energy ω^{exp}. According to the optical selection

#153227 - $15.00 USD Received 22 Aug 2011; revised 8 Oct 2011; accepted 8 Oct 2011; published 1 Nov 2011

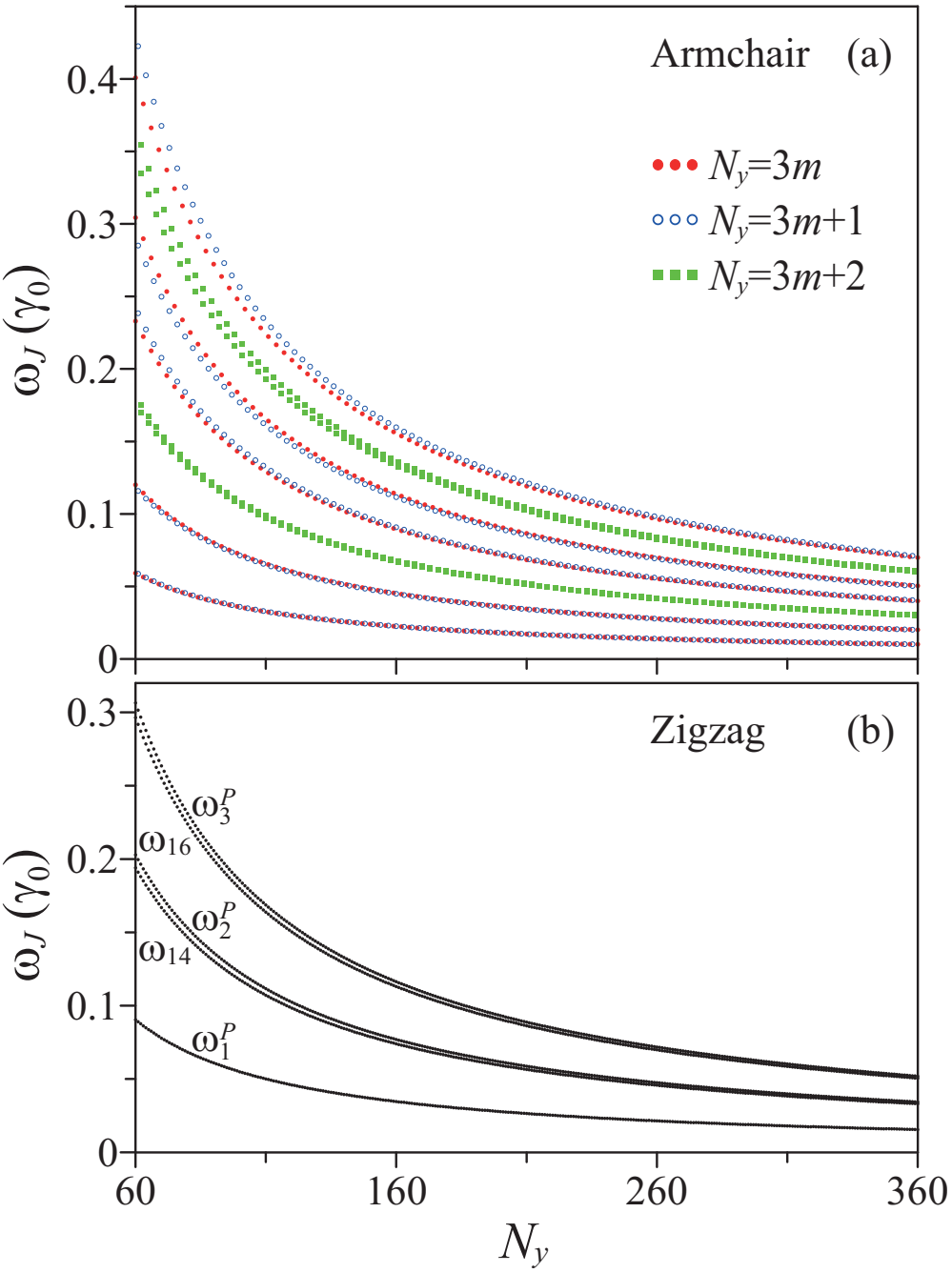

Fig. 5. The first five consecutive transition energies with respect to the ribbon width N_y for AGNR and ZGNR. The notations •, ○ and ■ correspond to AGNRs of $N_y = 3m$, $3m+1$, and $3m+2$, respectively.

#153227 - $15.00 USD Received 22 Aug 2011; revised 8 Oct 2011; accepted 8 Oct 2011; published 1 Nov 2011

rule, the measured peak positions $\omega_1^{P,exp}$, ω_{14}^{exp}, and ω_{16}^{exp} can be applied to specify the band-edge states $E_{J^c=2}^{edge}$, $E_{J^c=4}^{edge}$, and $E_{J^c=6}^{edge}$, respectively, which are the energy differences between the $J^c = even$ subband edges and the Fermi level. Moreover, the band-edge state energies of the $J^c = odd$ subbands are also obtainable, for example, $E_{J^c=3}^{edge} = \omega_2^{P,exp} - |E_{J^v=2}^{edge}| = \omega_2^{P,exp} - \omega_1^{P,exp}$. A similar backtracking strategy is valid for AGNRs based on the band symmetry about the Fermi energy. The band-edge state energy, which is half of the experimentally measured peak position, is given by $E_{J^c}^{edge} = |E_{J^v}^{edge}| = \omega_J^{exp}/2$, where $J^c = J^v = J$. Hence, the selection rule provides a way to overcome the disadvantages of optical measurements, which only yield information about the energy difference between two subbands.

6. Conclusion

We employ the tight-binding model to study the absorption spectra of GNRs. To our knowledge, this is the first time that the corresponding optical selection rules are analytically specified. The main results of this work are summarized as follows. First, the optical transition channels of absorption spectra for AGNRs and ZGNRs are exactly identified. Then, the characteristics of the absorption peaks, such as positions and heights relating to the energy dispersions, are discussed in detail. Most importantly, this work provides a theoretical explanation for the optical selection rules through analysis of the velocity matrix elements and the wavefunction features. The optical selection rules depend on the edge structure, i.e., armchair or zigzag edges. The selection rule of AGNRs ($\Delta J = 0$) has its origin in the relation between sublattices A and B within a certain state and the relation between the conduction and valence subenvelope functions of the same index, whereas the selection rule for ZGNRs ($|\Delta J| = odd$) is derived from the alternatively changing symmetry property with an increasing index. The quite different features of the wavefunctions for AGNRs and ZGNRs result in different selection rules. In addition, according to the selection rules, we can efficiently predict the peak positions and identify the corresponding transition channels. This gives us a way to overcome the limitations of optical measurements, and allows us to obtain exact energies of band-edge states.

Acknowledgments

One of us (H. C. Chung) wishes to thank M. H. Chung and S. M. Chen for financial support. This work was supported in part by the National Science Council of Taiwan under grant numbers NSC 99-2112-M-165-001-MY3 and 98-2112-M-006-013-MY4 and the National Center for Theoretical Sciences south (NCTS south).

#153227 - $15.00 USD Received 22 Aug 2011; revised 8 Oct 2011; accepted 8 Oct 2011; published 1 Nov 2011